

Pion properties at finite isospin chemical potential with isospin symmetry breaking^{*}

Zuqing Wu(吴祖庆)^{1;1)} Jialun Ping(平加伦)^{1;2)} Hongshi Zong(宗红石)^{2;3)}

¹ Department of Physics, Nanjing Normal University, Nanjing 210023, China

² Department of Physics, Nanjing University, Nanjing 210093, China

Abstract: Pion properties at finite temperature, finite isospin and baryon chemical potentials are investigated within the $SU(2)$ NJL model. In the mean field approximation for quarks and random phase approximation for mesons, we calculate the pion mass, the decay constant and the phase diagram with different quark masses for the u quark and d quark, related to QCD corrections, for the first time. Our results show an asymmetry between $\mu_I < 0$ and $\mu_I > 0$ in the phase diagram, and different values for the charged pion mass (or decay constant) and neutral pion mass (or decay constant) at finite temperature and finite isospin chemical potential. This is caused by the effect of isospin symmetry breaking, which is from different quark masses.

Keywords: finite temperature and finite isospin chemical potential, isospin symmetry breaking, properties of meson

PACS: 11.10.Wx, 12.38.-t, 25.75.Nq **DOI:** 10.1088/1674-1137/41/12/124106

1 Introduction

Quantum chromodynamics (QCD) [1, 2] is the basic theory of strong interactions. In the high-energy region, the momentum transfer in the processes is large and the coupling constant is small, so the processes can be treated perturbatively. However, in the low-energy region, the momentum transfer in the processes is small and the coupling constant is large, so one has to resort to nonperturbative methods and models. The Nambu–Jona-Lasinio (NJL) model [3, 4] is a well-known non-perturbative model which was proposed in 1961. One of the advantages of the NJL model is that it can exhibit the feature of dynamical chiral symmetry breaking [5]. Nevertheless, it is only an effective model of QCD, namely, neither confining nor renormalizable. Because of this shortcoming, a momentum cutoff is often introduced to avoid ultraviolet divergence.

Pion properties at finite temperature, baryon and isospin chemical potentials is an interesting topic [6, 7], and many authors have done research in this field. The masses and decay constants of neutral and/or charged pions have been investigated within the framework of the standard NJL model in Refs. [8–10]. The phases of a two-flavor NJL model at finite temperature, baryon and isospin chemical potentials have been studied by Bar-

ducci, Casalbuoni, Pettini, and Ravagli [11, 12]. Their study completes a previous analysis where only small isospin chemical potential μ_I was considered. The phase transition of QCD is investigated in Refs. [13–21]. Phase transition properties are studied under various conditions in Refs. [22–24]. The standard flavor $SU(2)$ NJL model was employed to numerically calculate pion superfluidity and its effect on meson properties and equations of state at finite temperature, isospin and baryon densities by He, Jin, and Zhuang [25].

The effects of isospin symmetry breaking from the different electric charges of u and d quarks relate to QED correction, and the difference in quark masses is related to QCD correction. First of all, the effect of the different quark masses is larger than electromagnetic effects in our study. This was found in Ref. [26] and Refs. [27, 28], where the Coulomb force is omitted in infinite systems. Besides, the electromagnetic effects within the NJL model have also been studied in many papers [29–32] and the calculation is complicated. So, for simplicity in this paper, as the first step, only the isospin symmetry breaking related to QCD correction is considered.

In our work, the two-flavor NJL model with mean field approximation is employed [33, 34]. In this framework, the meson modes are regarded as quantum fluctuations over the mean field, which can be calculated

Received 29 August 2017

^{*} Supported by National Natural Science Foundation of China (11175088, 11475085, 11535005, 11690030) and the Fundamental Research Funds for the Central Universities (020414380074)

1) E-mail: wujieyi1001@foxmail.com

2) E-mail: jlping@njnu.edu.cn

3) E-mail: zonghs@nju.edu.cn

©2017 Chinese Physical Society and the Institute of High Energy Physics of the Chinese Academy of Sciences and the Institute of Modern Physics of the Chinese Academy of Sciences and IOP Publishing Ltd

with the random phase approximation (RPA) [35]. In the present work, we focus on the case of different quark masses for u quark and d quark in the calculation of the masses and decay constants of the neutral and/or charged pions. The influence on the phase diagram of the mass difference between u quark and d quark is also studied.

The rest of this paper is organized as follows. In Section 2, the NJL model is briefly reviewed, and the mean field approximation is taken to treat the problems. In Section 3, we present the formalism of the pion mass and decay constant in the normal phase, then fix the parameters by fitting their values at zero temperature, zero baryon and isospin chemical potentials. In Section 4, the calculated neutral and/or charged pion masses in the superfluidity phase are presented and the phase diagram is drawn, with discussion. In the calculation, different effective quark masses are used for the u quark and d quark. Finally, a brief summary is given in the last section.

2 The Nambu–Jona-Lasinio model

In the present calculation, only two flavors are involved, $N_f=2$. The Lagrangian density of the NJL model for flavor $SU(2)$ is defined as [35–39]

$$\mathcal{L}=\bar{\psi}(i\gamma^\mu\partial_\mu-m_0)\psi+G\left[(\bar{\psi}\psi)^2+(\bar{\psi}i\gamma_5\boldsymbol{\tau}\psi)^2\right] \quad (1)$$

where pseudoscalar and scalar interactions correspond to π and σ excitations. Equivalently,

$$\begin{aligned} \mathcal{L} &= \bar{\psi}(i\gamma^\mu\partial_\mu-m_0)\psi+G\left[(\bar{\psi}\psi)^2\right. \\ &\quad \left.+2(\bar{\psi}i\gamma_5\boldsymbol{\tau}_+\psi)(\bar{\psi}i\gamma_5\boldsymbol{\tau}_-\psi)\right], \quad (2) \\ \tau_\pm &= (\tau_1\pm i\tau_2)/\sqrt{2} \end{aligned}$$

Here, π_- and π_+ replace π_1 and π_2 .

It has $U_B(1)\otimes SU_I(2)\otimes SU_A(2)$ symmetry, which is related to baryon number gauge symmetry, isospin symmetry and chiral symmetry separately, in the above Lagrangian density. However, $SU_I(2)$ isospin symmetry decomposes to the global symmetry $U_I(1)$, corresponding to a Bose-Einstein condensate of the charged pions, and $SU_A(2)$ chiral symmetry decomposes to $U_{IA}(1)$, corresponding to a chiral condensate of σ , when a nonzero isospin chemical potential appears.

Therefore, we introduce chiral condensation

$$\begin{aligned} \langle\bar{\psi}\psi\rangle &= \sigma=\sigma_u+\sigma_d, \\ \sigma_u &= \langle\bar{u}u\rangle, \\ \sigma_d &= \langle\bar{d}d\rangle, \end{aligned} \quad (3)$$

and the two pion condensations

$$\begin{aligned} \langle\bar{\psi}i\gamma_5\boldsymbol{\tau}_+\psi\rangle &= \sqrt{2}\langle\bar{u}i\gamma_5d\rangle=\pi^+, \\ \langle\bar{\psi}i\gamma_5\boldsymbol{\tau}_-\psi\rangle &= \sqrt{2}\langle\bar{d}i\gamma_5u\rangle=\pi^-. \end{aligned} \quad (4)$$

The σ condensate and π condensate are usually viewed as order parameters for the chiral and pion superfluidity phase transitions respectively.

In the mean field approximation, we adopt the following Lagrangian density

$$\begin{aligned} \mathcal{L}_{mf} &= \bar{\psi}[i\gamma^\mu\partial_\mu-(m_0-2G\sigma)+\mu\gamma_0+2G\pi i\gamma_5\boldsymbol{\tau}_1]\psi \\ &\quad -G(\sigma^2+\pi^2), \end{aligned} \quad (5)$$

where the matrix of the current quark mass is $m_0=(m_{0u},m_{0d})^T$. The matrix in flavor space for quark chemical potential is $\mu=\text{diag}(\mu_u,\mu_d)$,

$$\begin{aligned} \mu_u &= \frac{\mu_B}{3}+\frac{\mu_I}{2}, \\ \mu_d &= \frac{\mu_B}{3}-\frac{\mu_I}{2}, \end{aligned} \quad (6)$$

where μ_B and μ_I are the baryon and isospin chemical potentials.

In flavor space, the inverse of the quark propagator matrix can be written as

$$\mathcal{S}_{mf}^{-1}(p)=\begin{pmatrix} \gamma^\mu p_\mu+\mu_u\gamma_0-m_u & 2iG\pi\gamma_5 \\ 2iG\pi\gamma_5 & \gamma^\mu p_\mu+\mu_d\gamma_0-m_d \end{pmatrix} \quad (7)$$

where the quark mass

$$\begin{aligned} m_i &= m_{0i}-2G\langle\bar{\psi}\psi\rangle, \quad (i=u,d) \\ \langle\bar{\psi}\psi\rangle &= \langle\bar{u}u\rangle+\langle\bar{d}d\rangle. \end{aligned} \quad (8)$$

For the diagonal quark propagator matrix, only the chiral condensate is considered. It chooses a specific channel in the RPA through selecting the same polarization in bubble summation. Associated with self-polarization $\Pi_{MM}(k)$, it follows that [40, 41]

$$1-2G\Pi_{MM}(k)=0. \quad (9)$$

For the mean field propagator with off-diagonal components, such as the case of pion superfluidity, all related channels have to be taken into account in the RPA in summation of bubbles. The meson mode is

$$\det(1-2G\Pi(k))=0 \quad (10)$$

where $\Pi(k)$ is a 4×4 matrix for the four different types of channels [25].

We will discuss the properties of mesons in $\pi=0$ (normal phase) and in $\pi\neq 0$ (superfluid phase) respectively in the following.

3 Properties of mesons in normal phase

We first discuss the case of zero π condensation in the region of low μ_I . In this case, the inverse of the quark

propagator is

$$\mathcal{S}_{mf}^{-1}(p) = \begin{pmatrix} \gamma^\mu p_\mu + \mu_u \gamma_0 - m_u & 0 \\ 0 & \gamma^\mu p_\mu + \mu_d \gamma_0 - m_d \end{pmatrix}. \quad (11)$$

The quark propagator in the mean field in flavor space is diagonal and each element reads [35]

$$S_i(\vec{p}, \omega_n) = \frac{\not{p}_i + m_i}{2E_p^i} \frac{1}{i\omega_n - (E_p^i - \mu_i)} + \frac{\tilde{\not{p}}_i - m_i}{2E_p^i} \frac{1}{i\omega_n + (E_p^i + \mu_i)},$$

$$(E_p^i = \sqrt{\mathbf{p}^2 + m_i^2}, \quad i = u, d), \quad (12)$$

where

$$\not{p}_i = \gamma^0 E_p^i - \vec{\gamma} \cdot \vec{p}, \quad (13)$$

$$\tilde{\not{p}}_i = \gamma^0 E_p^i + \vec{\gamma} \cdot \vec{p}. \quad (14)$$

From the definitions of chiral condensations (3),

$$\sigma_u = -N_c \int \frac{d^4 p}{(2\pi)^4} \text{Tr}_D [i\mathcal{S}_u(p)],$$

$$\sigma_d = -N_c \int \frac{d^4 p}{(2\pi)^4} \text{Tr}_D [i\mathcal{S}_d(p)], \quad (15)$$

where Tr_D in Dirac space is taken.

Performing the trace of the quark propagators including energy projectors in Dirac space [42, 43], and the summation of Matsubara frequency [44, 45], we obtain

$$\sigma_i = -6 \int \frac{d^3 \mathbf{p}}{(2\pi)^3} \frac{m_i}{\sqrt{\mathbf{p}^2 + m_i^2}} (1 - f(E_i^-) - f(E_i^+)), \quad (i = u, d) \quad (16)$$

with quark energies

$$E_i^\pm(\mathbf{p}) = \sqrt{\mathbf{p}^2 + m_i^2} \pm \mu_i \quad (17)$$

where the Fermi-Dirac distribution function is

$$f(x) = \frac{1}{e^{\beta x} + 1}, \quad \beta = 1/T. \quad (18)$$

3.1 Pion masses at finite temperature and zero isospin chemical potential

In the normal phase without pion condensation, the polarization matrix $\Pi(k)$ is diagonal at finite isospin chemical potential corresponding to the basis $(\sigma, \pi_+, \pi_-, \pi_0)$. That is, $\sigma, \pi_+, \pi_-, \pi_0$ are the eigen collective modes in the normal phase. Therefore, the dispersion relation is resolved using Eq. (9) for each mode. The definition of the mass of the meson is the root k_0 at $\mathbf{k} = 0$.

The trace in color and flavor spaces is done, and polarization functions consisting of the propagator matrix elements are obtained,

$$\Pi_{\pi_0 \pi_0}(k) = -iN_c \int \frac{d^4 p}{(2\pi)^4} \text{Tr}_D \left(\gamma_5 \mathcal{S}_u(p+k) \gamma_5 \mathcal{S}_u(p) \right. \\ \left. + \gamma_5 \mathcal{S}_d(p+k) \gamma_5 \mathcal{S}_d(p) \right),$$

$$\Pi_{\pi_+ \pi_+}(k) = -2iN_c \int \frac{d^4 p}{(2\pi)^4} \text{Tr}_D \left(\gamma_5 \mathcal{S}_u(p+k) \gamma_5 \mathcal{S}_d(p) \right),$$

$$\Pi_{\pi_- \pi_-}(k) = -2iN_c \int \frac{d^4 p}{(2\pi)^4} \text{Tr}_D \left(\gamma_5 \mathcal{S}_d(p+k) \gamma_5 \mathcal{S}_u(p) \right), \quad (19)$$

Tr_D is now taken in spin space.

We use the quark propagator Eq. (12), then do the trace in spin space and the summation of the Matsubara frequency. The functions of meson polarization at $\mathbf{k} = 0$ are explicitly expressed as

$$\Pi_{\pi_+ \pi_+}(k_0) = -2N_c \int \frac{d^3 \mathbf{p}}{(2\pi)^3} \left[a^+ \left(\frac{1}{E_{ud,-}^- - k_0} (f(E_d^-) - f(E_u^-)) + \frac{1}{E_{du,-}^+ - k_0} (f(E_u^+) - f(E_d^+)) \right) \right. \\ \left. + a^- \left(\frac{1}{E_{ud,+}^- - k_0} (1 - f(E_u^-) - f(E_d^+)) + \frac{1}{E_{du,+}^+ + k_0} (1 - f(E_d^-) - f(E_u^+)) \right) \right], \quad (20)$$

$$\Pi_{\pi_- \pi_-}(k_0) = -2N_c \int \frac{d^3 \mathbf{p}}{(2\pi)^3} \left[a^+ \left(\frac{1}{E_{du,-}^- - k_0} (f(E_u^-) - f(E_d^-)) + \frac{1}{E_{ud,-}^+ - k_0} (f(E_d^+) - f(E_u^+)) \right) \right. \\ \left. + a^- \left(\frac{1}{E_{du,+}^- - k_0} (1 - f(E_d^-) - f(E_u^+)) + \frac{1}{E_{ud,+}^+ + k_0} (1 - f(E_u^-) - f(E_d^+)) \right) \right], \quad (21)$$

$$\Pi_{\pi_0 \pi_0}(k_0) = -N_c \int \frac{d^3 \mathbf{p}}{(2\pi)^3} \left[a_u^- \left(\frac{1}{2E_p^u - k_0} + \frac{1}{2E_p^u + k_0} \right) (1 - f(E_u^-) - f(E_u^+)) \right. \\ \left. + a_d^- \left(\frac{1}{2E_p^d - k_0} + \frac{1}{2E_p^d + k_0} \right) (1 - f(E_d^-) - f(E_d^+)) \right], \quad (22)$$

where

$$a^\pm = -E_p^u E_p^d \pm \mathbf{p}^2 \pm m_u m_d, \quad a_{u/d}^- = -E_p^{u/d} E_p^{u/d} - \mathbf{p}^2 - m_{u/d}^2;$$

$$E_p^{u/d} = \sqrt{\mathbf{p}^2 + m_{u/d}^2}, \quad E_{u/d}^\pm = \sqrt{\mathbf{p}^2 + m_{u/d}^2} \pm \mu_{u/d};$$

$$E_{i,j,\pm} = E_i \pm E_j, \quad E_{i,j,\pm}^\mp = E_i^\pm \pm E_j^\mp, \quad i, j = u, d.$$

Equations (8), (9), (16) and the pion decay constant (23) form a set of self-consistent equations. In this paper, we take a regularization-scheme-dependent cutoff $\Lambda = 571$ MeV. This and the other three model parameters, the coupling strength $G = 5.78 \times 10^{-6} \text{MeV}^{-2}$, the current quark mass, $m_{0u} = 4$ MeV, $m_{0d} = 13$ MeV, can be fixed by fitting the pion mass $m_{\pi^0} = 136$ MeV, $m_{\pi^\pm} = 139$ MeV, the pion decay constant $f_{\pi^0} = 93$ MeV, and the quark condensate $\sigma_0 = 2(-250)^3 \text{MeV}^3$ at zero temperature and zero chemical potential.

The neutral and/or charged pion masses at finite temperature are obtained by solving the above self-consistent equations in the case of $\mu_I = \mu_B = 0$. We can see in Fig. 1 that the masses of the neutral and charged pion both stay constant as the temperature increases at the beginning, and then increase with increasing temperature. Although the behavior of their masses with temperature is similar, there is a difference in their values, since the isospin symmetry breaking effect of the mass difference of the u and d quarks involves QCD correction. The curve of m_{π^+} with temperature is almost the same as that of m_{π^-} , because we do not consider the effects of the electromagnetic interaction.

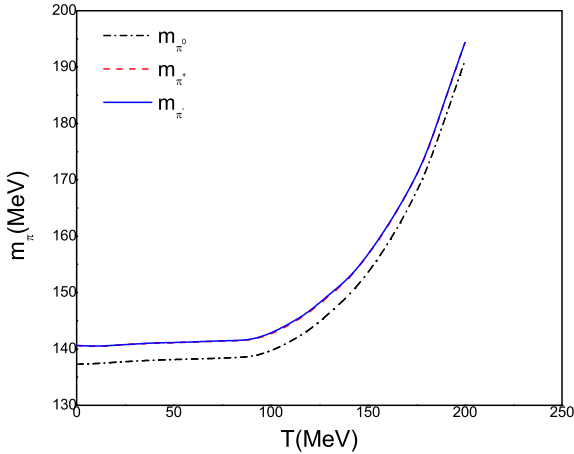


Fig. 1. (color online) Masses of the neutral and/or charged pions at finite temperature ($\mu_I = \mu_B = 0$).

3.2 Gell-Mann, Oakes, and Renner relation

The pion decay constant can be calculated by the Gell-Mann, Oakes, and Renner relation, which is the lowest-order approximation to the current algebraic result [36],

$$m_\pi^2 f_\pi^2 = \frac{-1}{2} (m_u + m_d) \langle \bar{\psi} \psi \rangle. \quad (23)$$

The above equation shows the relation between the experimental values – the pion masses and decay constants – and the theoretical parameters – the quark masses and quark condensate. Using Eq. (23), we plot the decay constant as shown in Fig. 2.

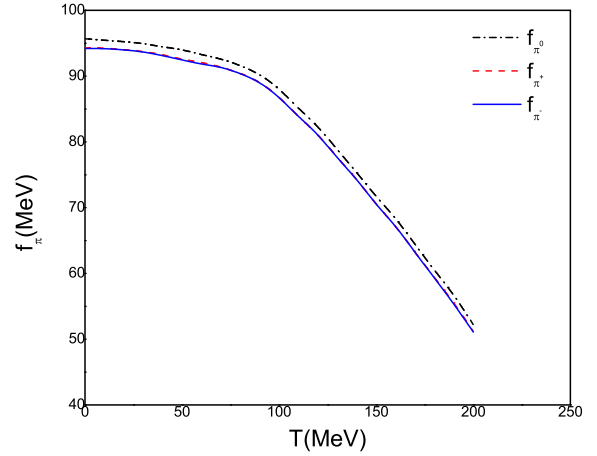


Fig. 2. (color online) Decay constants of the neutral or/and charged pions at finite temperature ($\mu_I = \mu_B = 0$).

Figure 2 shows that the decay constants of the neutral and charged pions both decrease with increasing temperature, but their values at any given temperature are different. This further illustrates the isospin symmetry breaking effect of $m_u \neq m_d$, which not only causes the mass difference of the neutral and charged pions at finite temperature, but also causes the difference in their decay constants. The behavior of f_{π^+} and f_{π^-} with temperature is almost the same, as the electromagnetic interaction is not considered.

4 Properties of mesons in superfluid phase

In the following, the case of nonzero π condensation is discussed. By the massive energy projectors [46, 47], the quark propagator in the mean field is explicitly given as

$$S_{mf}(p) = \begin{pmatrix} \mathcal{S}_{uu}(p) & \mathcal{S}_{ud}(p) \\ \mathcal{S}_{du}(p) & \mathcal{S}_{dd}(p) \end{pmatrix} \quad (24)$$

and the four elements of the matrix are

$$\mathcal{S}_{uu}(p) = \frac{p_0 - E_d^+}{(p_0 + E_u^+)(p_0 - E_d^+) - 4G^2\pi^2} \Lambda_-^u \gamma_0$$

$$+ \frac{p_0 + E_d^-}{(p_0 - E_u^-)(p_0 + E_d^-) - 4G^2\pi^2} \Lambda_+^u \gamma_0,$$

$$\mathcal{S}_{dd}(p) = \frac{p_0 - E_u^+}{(p_0 + E_d^+)(p_0 - E_u^+) - 4G^2\pi^2} \Lambda_-^d \gamma_0$$

$$+ \frac{p_0 + E_u^-}{(p_0 - E_d^-)(p_0 + E_u^-) - 4G^2\pi^2} \Lambda_+^d \gamma_0,$$

$$\begin{aligned}
 \mathcal{S}_{ud}(p) &= \frac{2iG\pi}{(p_0+E_u^+)(p_0-E_d^+)-4G^2\pi^2} A_+^d \gamma_5 \\
 &\quad + \frac{2iG\pi}{(p_0-E_u^-)(p_0+E_d^-)-4G^2\pi^2} A_-^u \gamma_5, \\
 \mathcal{S}_{du}(p) &= \frac{2iG\pi}{(p_0+E_d^+)(p_0-E_u^+)-4G^2\pi^2} A_+^u \gamma_5 \\
 &\quad + \frac{2iG\pi}{(p_0-E_d^-)(p_0+E_u^-)-4G^2\pi^2} A_-^d \gamma_5, \quad (25)
 \end{aligned}$$

with the energy projectors

$$A_{\pm}^i(\mathbf{p}) = \frac{1}{2} \left(1 \pm \frac{\gamma_0(\boldsymbol{\gamma} \cdot \mathbf{p} + m_i)}{E_p^i} \right), \quad (i=u,d).$$

From the definitions of the two pion condensations (4) and chiral condensation (3),

$$\begin{aligned}
 \sigma_u &= -N_c \int \frac{d^4p}{(2\pi)^4} \text{Tr}_D [i\mathcal{S}_{uu}(p)], \\
 \sigma_d &= -N_c \int \frac{d^4p}{(2\pi)^4} \text{Tr}_D [i\mathcal{S}_{dd}(p)], \\
 \pi &= N_c \int \frac{d^4p}{(2\pi)^4} \text{Tr}_D [(\mathcal{S}_{ud}(p) + \mathcal{S}_{du}(p))\gamma_5]. \quad (26)
 \end{aligned}$$

4.1 Phase diagram

Solving the chiral condensation σ and pion condensation π in the normal phase and in the superfluid phase respectively, σ and π as functions of μ_I in the case of zero temperature, plotted in Fig. 3, are both symmetric between $\mu_I > 0$ and $\mu_I < 0$. The critical μ_I for π is still exactly equal to the charged pion mass (139 MeV in our work, see Fig. 3 at zero temperature) even in the presence of unequal u and d quark masses.

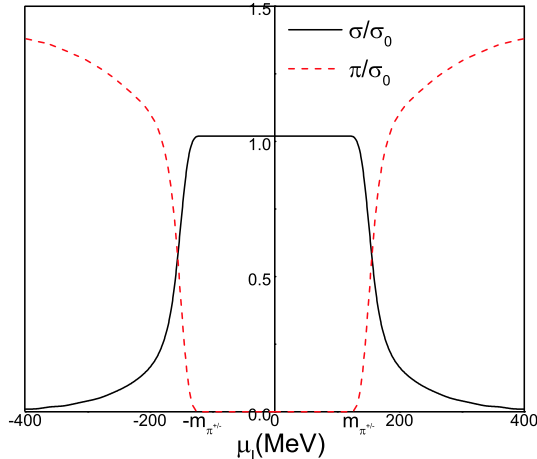


Fig. 3. (color online) Chiral condensation σ and pion condensation π scaled by σ_0 (the condensate at zero temperature and zero chemical potential) at μ_I ($T=\mu_B=0$).

The solution for π of Eq. (A3) divides $\pi=0$ (isospin symmetry restoration) from $\pi \neq 0$ (symmetry breaking).

The line of phase transition delimiting the above two regions is drawn in the $T-\mu_I$ plane ($\mu_B=0$) in Fig. 4.

In the real world, for the nonzero bare quark mass, the system is in the isospin symmetric phase ($\pi=0$) at high enough temperature, regardless of the value of the isospin chemical potential. At low temperature, however, the system is in the isospin symmetric phase only at low isospin chemical potential [11, 48].

In Fig. 4, the solid line shows the phase transition line in the case of $m_{0u} \neq m_{0d}$. When setting $m_{0u}=m_{0d}=(4+13)/2=8.5$ MeV, the dashed line is drawn in the $T-\mu_I$ plane. From the phase diagram, we can see: (1) in the $T-\mu_I$ plane, the dashed line is above the solid line; and (2) the dashed line is symmetrical between the regions of $\mu_I < 0$ and $\mu_I > 0$, while the solid line is asymmetrical. The discrepancy of the solution for π of Eq. (A3), related to the u and d quark between positive and negative isospin chemical potentials, arises from the different masses of the u and d quark in the calculation. This causes the asymmetry of the phase diagram, which is the effect of the isospin symmetry breaking associated with QCD correction ($m_u \neq m_d$) on the phase diagram.

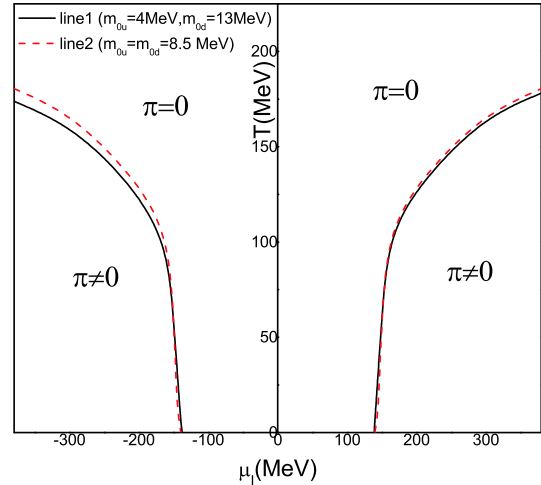


Fig. 4. (color online) Phase diagram in the $T-\mu_I$ plane ($\mu_B=0$).

4.2 Pion masses at finite isospin chemical potential

In the superfluid phase ($\pi \neq 0$), i.e. the quark propagator in the mean field with the off-diagonal elements of the matrix, the eigen collective modes for the system are not the original modes ($\sigma, \pi_+, \pi_-, \pi_0$) but rather a mixture of them. Through the quark propagator Eq. (25), the modes of the mesons are given by Eq. (10) with the polarization matrix $\Pi(k)$.

In the superfluid phase, the eigen collective modes are not σ, π_+ and π_- , because of the pion condensate. There is still no mixture between other mesons and π_0 ,

$$\Pi_{\pi_0\sigma}(k) = \Pi_{\pi_0\pi_+}(k) = \Pi_{\pi_0\pi_-}(k) = 0, \quad (27)$$

so the π_0 mass is determined by

$$1 - 2G\Pi_{\pi_0\pi_0}(k_0 = m_{\pi_0}, \mathbf{k} = 0) = 0. \quad (28)$$

The masses of the other mesons are determined by

$$\det \begin{pmatrix} 1 - 2G\Pi_{\sigma\sigma} & -2G\Pi_{\sigma\pi_+} & -2G\Pi_{\sigma\pi_-} \\ -2G\Pi_{\pi_+\sigma} & 1 - 2G\Pi_{\pi_+\pi_+} & -2G\Pi_{\pi_+\pi_-} \\ -2G\Pi_{\pi_-\sigma} & -2G\Pi_{\pi_-\pi_+} & 1 - 2G\Pi_{\pi_-\pi_-} \end{pmatrix}_{k_0=m} = 0 \quad (29)$$

at $\mathbf{k} = 0$, that is,

$$\begin{aligned} & \left[\left((1 - 2G\Pi_{\pi_+\pi_+}(k_0))(1 - 2G\Pi_{\pi_-\pi_-}(k_0)) \right. \right. \\ & - 4G^2\Pi_{\pi_+\pi_-}^2(k_0) \left. \left. \right) (1 - 2G\Pi_{\sigma\sigma}(k_0)) \right. \\ & - 16G^3\Pi_{\sigma\pi_+}(k_0)\Pi_{\sigma\pi_-}(k_0)\Pi_{\pi_+\pi_-}(k_0) \\ & - 4G^2\Pi_{\sigma\pi_-}^2(k_0)(1 - 2G\Pi_{\pi_+\pi_+}(k_0)) \\ & \left. \left. - 4G^2\Pi_{\sigma\pi_+}^2(k_0)(1 - 2G\Pi_{\pi_-\pi_-}(k_0)) \right]_{k_0=m} = 0. \quad (30) \end{aligned}$$

In the real world, for the nonzero bare quark mass, the mixture is not only between charged pions, but also between charged pions and σ . The mixture of $\pi-\pi$ is much stronger than the mixture of $\sigma-\pi$ [49, 50]. If the mixture of $\sigma-\pi$ is neglected in the superfluid phase [25], the σ meson is still the eigen mode, and its mass can be calculated from

$$1 - 2G\Pi_{\sigma\sigma}(k_0 = m_{\sigma}, \mathbf{k} = 0) = 0. \quad (31)$$

The masses of π_+ and π_- are calculated by the equation

$$\left[(1 - 2G\Pi_{\pi_+\pi_+}(k_0))(1 - 2G\Pi_{\pi_-\pi_-}(k_0)) - 4G^2\Pi_{\pi_+\pi_-}^2(k_0) \right]_{k_0=m} = 0. \quad (32)$$

The phase diagram at low temperatures in Fig. 4 shows that the system is in the normal phase in the beginning, then it changes from the normal phase ($\pi = 0$) to the superfluid phase ($\pi \neq 0$) as the isospin chemical potential increases, since pion condensation ($\pi \neq 0$) occurs with the increasing isospin chemical potential. Therefore, the pion masses can be calculated in both the normal phase and superfluid phase.

In the normal phase, the pion masses are determined by Eq. (9). In the superfluid phase, the pion masses are calculated through solving Eq. (28), together with Eq. (32), which are functions of μ_I at $T = 100$ MeV, $\mu_B = 0$. The numerical results are shown in Fig. 5. This shows the behavior of the neutral and/or charged pion masses at finite isospin chemical potential in the normal phase and in the superfluid phase separately.

The full calculation is plotted in Fig. 6, obtained by solving Eq. (30) in the superfluid phase. The $\sigma-\pi$ mixture is considered in this calculation, leading to the

difference in m_{π^-} compared to the results from the approximate calculation. The value of m_{π^-} is lower than that in the approximation.

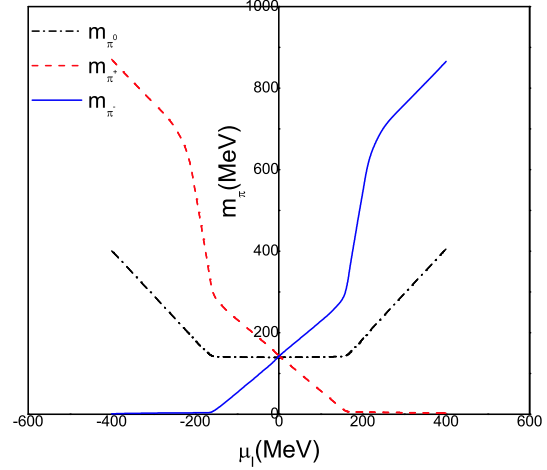


Fig. 5. (color online) Masses of the neutral and/or charged pions at finite isospin chemical potential (approximation neglecting $\sigma-\pi$ mixture) ($T = 100$ MeV, $\mu_B = 0$).

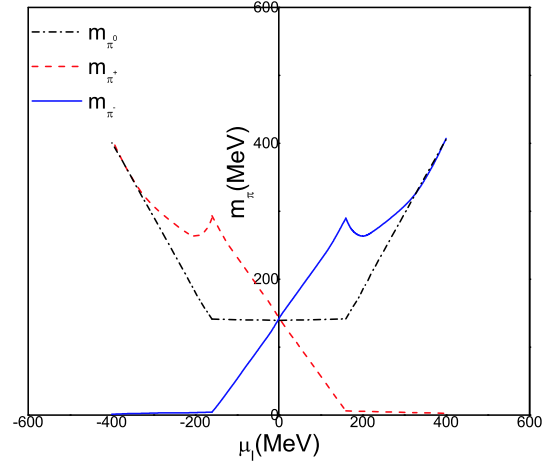


Fig. 6. (color online) Masses of the neutral and/or charged pions at finite isospin chemical potential (full calculation) ($T = 100$ MeV, $\mu_B = 0$).

Figures 5 and 6 both show that the curve of the positive (or negative) pion mass is asymmetric between the regions of $\mu_I < 0$ and $\mu_I > 0$, while that of the neutral pion mass is symmetric. There is also a slight asymmetry between the positive (or negative) pion mass in the region of $\mu_I < 0$ and the negative (or positive) pion mass in the region of $\mu_I > 0$. The isospin symmetry breaking effect of $m_u \neq m_d$ with QCD correction is considered in our calculation. For the case of $m_u = m_d$, readers can refer to Fig. 15. in Ref. [25].

5 Summary

In this paper, we numerically calculate the pion masses, the decay constants and the phase diagram at finite temperature and finite isospin chemical potential with different u- and d-quark masses in the mean field approximation of the 2-flavour NJL model for the first time. The results of our calculations indicate an asymmetry in the phase diagram and in the $m_\pi - \mu_I$ dia-

gram related to the charged pions, and different values for charged pion mass (or decay constant) and neutral pion mass (or decay constant) at finite temperature, as we consider the QCD correction of $m_u \neq m_d$ with isospin symmetry breaking. The results are different from $m_u = m_d$. Furthermore, we can also extend our calculation to the $SU(3)$ NJL model and calculate, for instance, properties of kaons [12, 51] or other mesons at finite temperature and finite isospin chemical potential.

Appendix A

Performing the trace in Dirac space and the summation of Matsubara frequency on Eq. (26), we have

$$\begin{aligned} \sigma_u = & -N_c \int \frac{d^3\mathbf{p}}{(2\pi)^3} \left(\frac{m_u}{E_u} \right) \left[\left(\frac{-1}{E_2^+ - E_2^-} \right) \left((E_2^+ - E_d^+) (1 - 2f(E_2^+)) - (E_2^- - E_d^+) \right. \right. \\ & \left. \left. + (1 - 2f(E_2^-)) \right) \left(\frac{1}{E_4^+ - E_4^-} \right) \left((E_4^+ + E_d^-) (1 - 2f(E_4^+)) - (E_4^- + E_d^-) (1 - 2f(E_4^-)) \right) \right], \end{aligned} \quad (\text{A1})$$

$$\begin{aligned} \sigma_d = & -N_c \int \frac{d^3\mathbf{p}}{(2\pi)^3} \left(\frac{m_d}{E_d} \right) \left[\left(\frac{-1}{E_1^+ - E_1^-} \right) \left((E_1^+ - E_u^+) (1 - 2f(E_1^+)) - (E_1^- - E_u^+) \right. \right. \\ & \left. \left. + (1 - 2f(E_1^-)) \right) \left(\frac{1}{E_3^+ - E_3^-} \right) \left((E_3^+ + E_u^-) (1 - 2f(E_3^+)) - (E_3^- + E_u^-) (1 - 2f(E_3^-)) \right) \right], \end{aligned} \quad (\text{A2})$$

$$\begin{aligned} \pi = & 4N_c G \pi \int \frac{d^3\mathbf{p}}{(2\pi)^3} \left[\frac{1}{E_1^+ - E_1^-} (f(E_1^+) - f(E_1^-)) + \frac{1}{E_2^+ - E_2^-} (f(E_2^-) - f(E_2^+)) \right. \\ & \left. + \frac{1}{E_3^+ - E_3^-} (f(E_3^-) - f(E_3^+)) + \frac{1}{E_4^+ - E_4^-} (f(E_4^-) - f(E_4^+)) \right], \end{aligned} \quad (\text{A3})$$

where

$$\begin{aligned} E_1^\pm &= \frac{-\Delta_1 \pm \sqrt{\Delta_1^2 + 4(E_d^+ E_u^+ + 4G^2 \pi^2)}}{2}, \\ E_2^\pm &= \frac{\Delta_1 \pm \sqrt{\Delta_1^2 + 4(E_d^+ E_u^+ + 4G^2 \pi^2)}}{2}, \\ E_3^\pm &= \frac{-\Delta_2 \pm \sqrt{\Delta_2^2 + 4(E_d^- E_u^- + 4G^2 \pi^2)}}{2}, \\ E_4^\pm &= \frac{\Delta_2 \pm \sqrt{\Delta_2^2 + 4(E_d^- E_u^- + 4G^2 \pi^2)}}{2}, \\ E_u &= \sqrt{m_u^2 + \mathbf{p}^2}, \\ E_d &= \sqrt{m_d^2 + \mathbf{p}^2}, \\ \Delta_1 &= E_d^+ - E_u^+, \\ \Delta_2 &= E_u^- - E_d^-. \end{aligned} \quad (\text{A4})$$

After doing the trace and performing the summation of Mastubara frequency, the functions of meson polarization in Eq. (28) and Eq. (32) at $\mathbf{k}=0$ are explicitly expressed as

$$\begin{aligned}
 \Pi_{\pi_+\pi_+}(k) = & -N_c \int \frac{d^3\mathbf{p}}{(2\pi)^3} \left[B_{1u}^+ (b^+ F_{1d2}^+ + b^- G_{1d4}^+) (1-2f(E_1^+)) + B_{1u}^- (b^+ F_{1d2}^- + b^- G_{1d4}^-) (1-2f(E_1^-)) \right. \\
 & + B_{2d}^+ (b^+ f_{2u1}^+ + b^- g_{2u3}^+) (1-2f(E_2^+)) + B_{2d}^- (b^+ f_{2u1}^- + b^- g_{2u3}^-) (1-2f(E_2^-)) \\
 & + C_{3u}^+ (b^- F_{3d2}^+ + b^+ G_{3d4}^+) (1-2f(E_3^+)) + C_{3u}^- (b^- F_{3d2}^- + b^+ G_{3d4}^-) (1-2f(E_3^-)) \\
 & + \left(C_{4d}^+ + \frac{k_0}{E_{44,-}^{+,+}} \right) \left(\left(b^- f_{4u1}^+ + \frac{b^- k_0}{(E_{41,-}^{+,+} - k_0)(E_{41,-}^{+,-} - k_0)} \right) \right. \\
 & + \left. \left(b^+ g_{4u3}^+ + \frac{b^+ k_0}{(E_{43,-}^{+,+} - k_0)(E_{43,-}^{+,-} - k_0)} \right) \right) (1-2f(E_4^+)) \\
 & + \left(C_{4d}^- + \frac{k_0}{E_{44,-}^{-,+}} \right) \left(\left(b^- f_{4u1}^- + \frac{b^- k_0}{(E_{41,-}^{-,+} - k_0)(E_{41,-}^{-,-} - k_0)} \right) \right. \\
 & + \left. \left(b^+ g_{4u3}^- + \frac{b^+ k_0}{(E_{43,-}^{-,+} - k_0)(E_{43,-}^{-,-} - k_0)} \right) \right) (1-2f(E_4^-)) \left. \right], \tag{A5}
 \end{aligned}$$

$$\begin{aligned}
 \Pi_{\pi_-\pi_-}(k) = & -N_c \int \frac{d^3\mathbf{p}}{(2\pi)^3} \left[B_{1u}^+ (b^+ f_{1d2}^+ + b^- g_{1d4}^+) (1-2f(E_1^+)) + B_{1u}^- (b^+ f_{1d2}^- + b^- g_{1d4}^-) (1-2f(E_1^-)) \right. \\
 & + B_{2d}^+ (b^+ F_{2u1}^+ + b^- G_{2u3}^+) (1-2f(E_2^+)) + B_{2d}^- (b^+ F_{2u1}^- + b^- G_{2u3}^-) (1-2f(E_2^-)) \\
 & + \left(C_{3u}^+ + \frac{k_0}{E_{33,-}^{+,+}} \right) \left(\left(b^- f_{3d2}^+ + \frac{b^- k_0}{(E_{32,-}^{+,+} - k_0)(E_{32,-}^{+,-} - k_0)} \right) \right. \\
 & + \left. \left(b^+ g_{3d4}^+ + \frac{b^+ k_0}{(E_{34,-}^{+,+} - k_0)(E_{34,-}^{+,-} - k_0)} \right) \right) (1-2f(E_3^+)) \\
 & + \left(C_{3u}^- + \frac{k_0}{E_{33,-}^{-,+}} \right) \left(\left(b^- f_{3d2}^- + \frac{b^- k_0}{(E_{32,-}^{-,+} - k_0)(E_{32,-}^{-,-} - k_0)} \right) \right. \\
 & + \left. \left(b^+ g_{3d4}^- + \frac{b^+ k_0}{(E_{34,-}^{-,+} - k_0)(E_{34,-}^{-,-} - k_0)} \right) \right) (1-2f(E_3^-)) \\
 & + C_{4d}^+ (b^- F_{4u1}^+ + b^+ G_{4u3}^+) (1-2f(E_4^+)) + C_{4d}^- (b^- F_{4u1}^- + b^+ G_{4u3}^-) (1-2f(E_4^-)) \left. \right], \tag{A6}
 \end{aligned}$$

$$\begin{aligned}
 \Pi_{\pi_+\pi_-}(k) = & -4N_c G^2 \pi^2 \int \frac{d^3\mathbf{p}}{(2\pi)^3} \left[D_2^+ (-2(H_2^+ + I_2^+) + a^+ (h_{24}^+ + i_{24}^+)) (1-2f(E_2^+)) \right. \\
 & + D_2^- (-2(H_2^- + I_2^-) + a^+ (h_{24}^- + i_{24}^-)) (1-2f(E_2^-)) \\
 & + D_4^+ (-2(H_4^+ + I_4^+) + a^+ (h_{42}^+ + i_{42}^+)) (1-2f(E_4^+)) \\
 & + D_4^- (-2(H_4^- + I_4^-) + a^+ (h_{42}^- + i_{42}^-)) (1-2f(E_4^-)) \left. \right], \tag{A7}
 \end{aligned}$$

$$\begin{aligned}
 \Pi_{\pi_0\pi_0}(k) = & N_c \int \frac{d^3\mathbf{p}}{(2\pi)^3} \left[D_1^+ (J_{1u3}^+ + K_{1u3}^+) (1-2f(E_1^+)) + D_1^- (J_{1u3}^- + K_{1u3}^-) (1-2f(E_1^-)) \right. \\
 & + D_2^+ (J_{2d4}^+ + K_{2d4}^+) (1-2f(E_2^+)) + D_2^- (J_{2d4}^- + K_{2d4}^-) (1-2f(E_2^-)) \\
 & + D_3^+ (j_{3u1}^+ + k_{3u1}^+) (1-2f(E_3^+)) + D_3^- (j_{3u1}^- + k_{3u1}^-) (1-2f(E_3^-)) \\
 & + D_4^+ (j_{4d2}^+ + k_{4d2}^+) (1-2f(E_4^+)) + D_4^- (j_{4d2}^- + k_{4d2}^-) (1-2f(E_4^-)) \left. \right]. \tag{A8}
 \end{aligned}$$

Here

$$\begin{aligned}
 B_{ij}^\pm &= \frac{E_{ij,-}^{\pm,+}}{E_{ii,-}^{\pm,\mp}}, \quad C_{ij}^\pm = \frac{E_{ij,+}^{\pm,-}}{E_{ii,-}^{\pm,\mp}}, \quad D_i^\pm = \frac{1}{E_{ii,-}^{\pm,\mp}}, \\
 F_{ijk}^\pm &= \frac{E_{ij,-}^{\pm,+} + k_0}{(E_{ik,-}^{\pm,+} + k_0)(E_{ik,-}^{\pm,-} + k_0)}, \\
 f_{ijk}^\pm &= \frac{E_{ij,-}^{\pm,+} - k_0}{(E_{ik,-}^{\pm,+} - k_0)(E_{ik,-}^{\pm,-} - k_0)},
 \end{aligned}$$

$$\begin{aligned}
 G_{ijk}^{\pm} &= \frac{E_{ij,+}^{\pm,-} + k_0}{(E_{ik,-}^{\pm,+} + k_0)(E_{ik,-}^{\pm,-} + k_0)}, & j_{ijk}^{\pm} &= \frac{E_{ij,-}^{\pm,+}(E_{ij,+}^{\pm,-} + k_0)}{(E_{ik,-}^{\pm,+} - k_0)(E_{ik,-}^{\pm,-} - k_0)}, \\
 g_{ijk}^{\pm} &= \frac{E_{ij,+}^{\pm,-} - k_0}{(E_{ik,-}^{\pm,+} - k_0)(E_{ik,-}^{\pm,-} - k_0)}, & K_{ijk}^{\pm} &= \frac{E_{ij,+}^{\pm,-}(E_{ij,-}^{\pm,+} - k_0)}{(E_{ik,-}^{\pm,+} + k_0)(E_{ik,-}^{\pm,-} + k_0)}, \\
 H_i^{\pm} &= \frac{1}{k_0(E_{ii,-}^{\pm,\mp} + k_0)}, \quad I_i^{\pm} = \frac{1}{-k_0(E_{ii,-}^{\pm,\mp} - k_0)}, & k_{ijk}^{\pm} &= \frac{E_{ij,+}^{\pm,-}(E_{ij,-}^{\pm,+} + k_0)}{(E_{ik,-}^{\pm,+} + k_0)(E_{ik,-}^{\pm,-} + k_0)}, \\
 h_{ik}^{\pm} &= \frac{1}{(E_{ik,-}^{\pm,+} + k_0)(E_{ik,-}^{\pm,-} + k_0)}, & i &= k=1,2,3,4, \quad j=u,d, \\
 i_{ik}^{\pm} &= \frac{1}{(E_{ik,-}^{\pm,+} - k_0)(E_{ik,-}^{\pm,-} - k_0)}, & b^{\pm} &= -1 \pm \frac{p^2 + m_u m_d}{E_p^u E_p^d}, \\
 J_{ijk}^{\pm} &= \frac{E_{ij,-}^{\pm,+}(E_{ij,+}^{\pm,-} - k_0)}{(E_{ik,-}^{\pm,+} - k_0)(E_{ik,-}^{\pm,-} - k_0)}, & E_{mn,\pm} &= E_m \pm E_n, \quad E_{mn,\pm}^{\pm,\mp} = E_m^{\pm} \pm E_n^{\mp}, \\
 & & m,n &= 1,2,3,4,u,d.
 \end{aligned} \tag{A9}$$

References

- 1 M. Asakawa and K. Yazaki, Nucl. Phys. A, **504**: 668 (1989)
- 2 S. Klimt, M. Lutz, and W. Weise, Phys. Lett. B, **249**: 386 (1990)
- 3 S. Roessner, T. Hell, C. Ratti et al, Nucl. Phys. A, **814**: 118 (2008)
- 4 K. Fukushima, Phys. Rev. D, **77**: 114028 (2008)
- 5 A. Barducci, R. Casalbuoni, S. De Curtis et al, Phys. Rev. D, **46**: 2203 (1992)
- 6 Zhao Zhang, Yu-Xin Liu, Phys. Rev. C, **75**: 064910 (2007)
- 7 Jens O. Andersen, Lars Kyllingstad, J. Phys. G, **37**: 015003 (2009)
- 8 C. Villavicencio, E.S. Fraga, Nucl. Phys. A, **785**: 238–240 (2007)
- 9 M. Loewe and C. Villavicencio, Phys. Rev. D, **67**: 074034 (2003); Phys. Rev. D, **70**: 074005 (2004)
- 10 M. Huang, P. Zhuang, and W. Chao, Phys. Rev. D, **67**: 065015 (2003)
- 11 A. Barducci, R. Casalbuoni, G. Pettini et al, Phys. Rev. D, **69**: 096004 (2004)
- 12 A. Barducci, R. Casalbuoni, G. Pettini et al, Phys. Rev. D, **71**: 016011 (2005)
- 13 Zan Pan, Zhu-Fang Cui, Chao-Hsi Chang et al, Int. J. Mod. Phys. A, **32**: 1750067 (2017)
- 14 Qing-Wu Wang, Zhu-Fang Cui, and Hong-Shi Zong, Phys. Rev. D, **94**: 096003 (2016)
- 15 Zhu-Fang Cui, Ian C. Cloet, Ya Lu et al, Phys. Rev. D, **94**: 071503 (2016)
- 16 Ya Lu, Zhu-Fang Cui, Zan Pan et al, Phys. Rev. D, **93**: 074037 (2016)
- 17 Yi-Lun Du, Zhu-Fang Cui, Yong-Hui Xia et al, Phys. Rev. D, **88**: 114019 (2013)
- 18 Hong-shi Zong and Wei-min Sun, Phys. Rev. D, **78**: 054001 (2008)
- 19 Guo-yun Shao, Lei Chang, Yu-xin Liu et al, Phys. Rev. D, **73**: 076003 (2006)
- 20 Gao-feng Sun, Lianyi He, and Pengfei Zhuang, Phys. Rev. D, **75**: 096004 (2007)
- 21 Lianyi He, Meng Jin, and Pengfei Zhuang, Phys. Rev. D, **74**: 036005 (2006)
- 22 Yu Jiang, Yuan-mei Shi, Hua Li et al, Phys. Rev. D, **78**: 116005 (2008)
- 23 Yu Jiang, Yuan-mei Shi, Hong-tao Feng et al, Phys. Rev. C, **78**: 025214 (2008)
- 24 Hongshi Zong, Xiaohua Wu, Xiaofu Lu et al, arXiv: hep-ph/0109112
- 25 Lianyi He, Meng Jin, and Pengfei Zhuang, Phys. Rev. D, **71**: 116001 (2005)
- 26 Nathan Isgur, Phys. Rev. D, **21**: 779 (1980); Phys. Rev. D, **23**: 817 (1981)
- 27 P. G. Reinhard, Rept. Prog. Phys., **52**: 439 (1989)
- 28 John Dirk Walecka, *Theoretical nuclear and subnuclear physics*, Second edition (World Scientific, 2004), p.18
- 29 Takahiro Fujihara, Tomohiro Inagaki, and Daiji Kimura, arXiv: hep-ph/0702160
- 30 Takahiro Fujihara, Tomohiro Inagaki, and Daiji Kimura, arXiv: hep-ph/0511218
- 31 Shane Drury, Thomas Blum, Masashi Hayakawa et al, PoS LATTICE2013: 268 (2014)
- 32 Derek P. Horkel and Stephen R. Sharp, Phys. Rev. D, **92**: 074501 (2015)
- 33 B. Klein, D. Toublan, and J. J. M. Verbaarschot, arXiv: hep-ph/0405180
- 34 B. Klein, D. Toublan, and J. J. M. Verbaarschot, Phys. Rev. D, **68**: 014009 (2003)
- 35 S. P. Klevansky, Rev. Mod. Phys., **64**: 649 (1992)
- 36 Nambu and G. Jona-Lasinio, Phys. Rev., **122**: 345 (1961); **124**: 246 (1961)
- 37 U. Vogl and Weise, Prog. Part. and Nucl. Phys., **27**: 195 (1991)
- 38 M. K. Volkov, Phys. Part. Nucl., **24**: 35 (1993)
- 39 T. Hatsuda and T. Kunihiro, Phys. Rep., **247**: 221 (1994)
- 40 J. Hufner, S. P. Klevansky, P. Zhuang et al, Ann. Phys. (N.Y.), **234**: 225 (1994)
- 41 P. Zhuang, J. Hufner, S. P. Klevansky, Nucl. Phys. A, **576**: 525 (1994)
- 42 Michael E. Peskin and Daniel V. Schroeder, *An introduction to quantum field*, (World Book Press, 2006)
- 43 W. Greiner, J. Reinhardt, *Quantum Electrodynamics*, (Springer-Verlag Berlin Heidelberg, 1992)
- 44 J. I. Kapusta and C. Gale, *Finite-temperature field theory: Principles and applications*, (Cambridge University Press, 2006)
- 45 Shusheng Xu, Yan Yan, Zhufang Cui et al, Int. J. Mod. Phys. A, **30**: 1550217 (2015)
- 46 M. Huang, P. Zhuang and W. Chao, Phys. Rev. D, **65**: 076012 (2002)
- 47 Z. G. Wang and S. L. Wan, and W. M. Yang, arXiv: hep-ph/0508302
- 48 Takahiro Sasaki, Yuji Sakai, Hiroaki Kouno et al, Phys. Rev. D, **82**: 116004 (2010)
- 49 M. Framk, M. Buballa, and M. Oertel, Phys. Lett. B, **562**: 221 (2003)
- 50 Xuewen Hao and Pengfei Zhuang, Phys. Lett. B, **652**: 275 (2007)
- 51 He Liu, Jun Xu, Lie-Wen Chen et al, Phys. Rev. D, **94**: 065032 (2016)